arXiv:2501.15194v1 [cs.LG] 25 Jan 2025

Reliable Pseudo-labeling via Optimal Transport with Attention for Short Text Clustering

Zhihao Yao [1] **Jixuan Yin** [1] **Bo Li** [1]

Abstract

Short text clustering has gained significant attention in the data mining community. However, the limited valuable information contained in short texts often leads to low-discriminative representations, increasing the difficulty of clustering. This paper proposes a novel short text clustering framework, called Reliable **P**seudo-labeling via **O**ptimal **T**ransport with **A**ttention for Short Text Clustering (**POTA**), that generate reliable pseudo-labels to aid discriminative representation learning for clustering. Specially, **POTA** first implements an instance-level attention mechanism to capture the semantic relationships among samples, which are then incorporated as a regularization term into an optimal transport problem. By solving this OT problem, we can yield reliable pseudo-labels that simultaneously account for sample-to-sample semantic consistency and sample-to-cluster global structure information. Additionally, the proposed OT can adaptively estimate cluster distributions, making **POTA** well-suited for varying degrees of imbalanced datasets. Then, we utilize the pseudo-labels to guide contrastive learning to generate discriminative representations and achieve efficient clustering. Extensive experiments demonstrate **POTA** outperforms state-of-the-art methods. The code is available at: https://github.com/YZH0905/POTA-STC/tree/main.

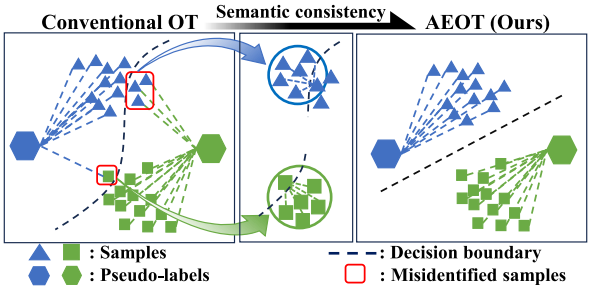

Figure 1: Schematic illustration of the motivation. Conventional OT only considers the sample-to-cluster relationship, causing similar and adjacent samples to be assigned different pseudo-labels (red boxes). Our proposed AEOT addresses this issue by incorporating sample-to-sample semantic consistency, which will producing more accurate pseudo-labels

1. Introduction

Text clustering is one of the key methods for organizing and summarizing large unstructured text datasets (Huang et al., 2022). Its primary objective is to group text data into different clusters without the help of supervised information, such that intra-cluster data are similar and inter-cluster data are distinct. Short text clustering, a subfield of text clustering, has garnered increasing attention in recent years due to the rise of social media platforms (Taherdoost, 2023), chatbots (Shum et al., 2018), and other technologies that generate vast amounts of short-form content. However, the short length of the text inherently limits the amount of semantic information it contains, resulting in low-discriminative representations when mapping text to the feature space, which makes short text clustering a challenging task. Therefore, extracting more distinctive representations is crucial in the research of short text clustering (Ahmed et al., 2022).

In unsupervised learning, pseudo-labels can guide the model to learn discriminative and robust representations (Gupta et al., 2020). Inspired by this, various techniques have been developed to generate more reliable pseudo-labels. Earlier methods heavily relied on the model predictions and used the argmax operation to generate pseudo-labels (Sohn et al., 2020). However, these methods generate pseudo-labels for per-sample independently, ignoring the global or local information of the sample distribution (Caron et al., 2020). Consequently, if the model's predictions contain slight errors (i.e., The probability assignment of the incorrect category is slightly higher than the correct category.), pseudo-labels will further mislead the model and amplify its bias. For previous limitations, Optimal Transport (OT) provides an effective solution by optimizing the overall cost of matching the sample distribution to the cluster distribution to generate pseudo-labels (Xia et al., 2022). In this way, the pseudo-labels incorporate the relationships between samples and clusters

[1]School of Harbin Engineering University, Institute of Intelligent Systems Science and Engineering, Harbin, China. Correspondence to: Zhihao Yao <15588333753@163.com>.

Preliminary work.

on the global scale, i.e., *sample-to-cluster global structure*. However, OT-based methods only consider the relationships from samples to clusters, neglecting the inherent semantic consistency between samples (Chang et al., 2023), i.e., *sample-to-sample semantic consistency*. This oversight can lead to misclassification at decision boundaries, resulting in adjacent and similar samples being assigned to different pseudo-labels, as shown in Figure 1.

To address the above issue, we integrate an instance-level attention mechanism into our proposed novel OT formulation to generate pseudo-labels, we refer to this OT formulation as *semantic-aware adaptive optimal transport* (**AEOT**). By solving the AEOT problem, we can get reliable pseudo-labels that simultaneously account sample-to-sample semantic consistency and sample-to-cluster global structure information. Additionally, AEOT can adaptively estimate class distributions, making our method well-suited for handling varying degrees of imbalance datasets. In our pseudo-labeling method, the attention mechanism and AEOT are iteratively reinforcing each other. Specifically, we first use the pseudo-labels generated by AEOT to guide the training of an attention network at the instance level of samples, which fully exploits the semantic similarity relationships between samples. Then, these similarity relationships are fed back into AEOT to enhance the effectiveness of pseudo-labels. The above iterative process starts with the use of K-means to generate pseudo-labels, and then forms a virtuous circle. In this circle, better pseudo-labels help establish enhanced semantic similarity relationships, which in turn facilitate the generation of more effective pseudo-labels.

Then, we use the pseudo-labels generated by AEOT to guide cluster-level contrastive learning, and combined it with instance-level contrastive learning to jointly enhance representation quality and improve clustering efficiency.

Note that our proposed AEOT is a novel OT formulation with a nonconvex objective function that cannot be solved using conventional OT methods. To this end, we propose a hyper-efficient solution that embeds the Lagrangian multiplier method (Bertsekas, 2014) within the generalized conditional gradient framework (Yu et al., 2017) to solve AEOT.

We summarize our main contributions as follows:

- We propose a progressively learning short text clustering formwork, the key idea is to iteratively perform pseudo-label generation process with semantic regularization and semantic construction process to produce reliable pseudo-labels, hence to provide optimal supervised guidance for enhancing clustering performance.
- We propose a novel pseudo-labeling method based on optimal transport, i.e., AEOT, which simultaneously considers sample-to-sample semantic consistency and sample-to-cluster global structure to generate superior pseudo-labels. Additionally, AEOT can adaptively estimate the class distribution, making it suitable for handling varying degrees of data imbalance.
- We propose using an instance-level attention mechanism to capture the semantic similarity relationships among samples with pseudo-label guidance, which will help to fully exploit superior similarity relationships.
- We conducted extensive experiments on eight benchmark datasets, and the results demonstrate that our method achieves state-of-the-art performance in the field of unsupervised short text clustering.

2. Related Work

2.1. Pseudo-labeling based on optimal transport

Optimal Transport is a mathematical theory focused on finding an efficient transport matrix from one distribution to another while minimizing the total transport cost (Peyré et al., 2019). Compared to conventional pseudo-labeling methods, the OT-based method considers the overall structure between sample distribution and cluster distribution to generate pseudo-labels, rather than relying heavily on each sample and proceeding independently (Berthelot et al., 2020; Xia et al., 2022). For example, SELA (Asano et al., 2020) employs a uniform distribution as a marginal constraint on the cluster datasets. However, this method is not suitable for imbalanced datasets. Subsequently, PPOT (Zhang et al., 2024) and RSTC (Zheng et al., 2023) incorporate the degree of imbalance of predicted cluster probabilities as a penalty term in the objective function, enabling these methods to be applied to imbalanced datasets. However, all of these OT-based methods only consider the relationships between sample and cluster, neglecting the inherent consistency between samples. In response to this limitation, CSOT (Chang et al., 2023) gives effective improvements by incorporating the cosine similarity between samples into the OT problem, thus embedding the inherent sample-to-sample consistency. However, using cosine similarity to measure relationships between samples has certain limitations. In addition, CSOT cannot handle unbalanced datasets.

In contrast to these methods, which either overlook sample-to-sample semantic consistency or fail on imbalanced datasets, our proposed AEOT addresses both issues. In AEOT, the sample-to-sample semantic consistency is derived not only from cosine similarity but also from similarities modeled through an attention mechanism. This enables more effective semantic consistency, thereby producing more reliable pseudo-labels.

2.2. Short Text Clustering

Previous research on short text clustering can be broadly divided into three categories: conventional methods, deep learning-based methods, and deep joint clustering methods. Conventional methods rely on vector space statistical techniques, such as BOW and TF-IDF, to extract text features (Chowdhury, 2010). However, the representations produced by these methods are typically sparse and lack semantic information. Deep learning-based methods use neural networks to extract text features and then apply metric methods, such as K-means, for clustering (Xu et al., 2017). However, the two components of these methods are often decoupled, which may result in representations extracted by the former being unsuitable for the latter. In recent years, deep joint clustering methods (Xie et al., 2016) have gained prominence by integrating representation learning and clustering into a unified framework, allowing the clustering objective to directly guide the representation learning process. Notable examples, including SCCL (Zhang et al., 2021) and RSTC (Zheng et al., 2023) have achieved good results in the field of short text clustering.

Among these methods, only RSTC uses pseudo-labels to help the model learn discriminative representations. Specifically, RSTC proposes an adaptive optimal transport formulation to generate pseudo-labels. However, the robustness of these pseudo-labels is limited due to the neglect of sample-to-sample information. In this paper, we propose a new formulation (AEOT) to generate reliable pseudo-labels, assisting the model to learn more efficient representations.

3. Method

3.1. Overall Structure of POTA

The overall structure of **POTA** is shown in Figure 2. It consists of three components: the Pseudo-label Generation Module (PGM), the Semantic Similarity Construction Module (SSCM), and the Contrastive Learning Module (CLM).

The PGM executes the AEOT problem constructed using the similarity matrix output by the SSCM to generate pseudo-labels. This pseudo-labels simultaneously consider both sample-to-cluster global structure and sample-to-sample semantic consistency information. The SSCM establishes an attention network at the instance level and trains it using pseudo-labels generated by the PGM as supervised information, thereby capturing more effective similarity relationships of samples. The CLM performs both cluster-level and instance-level contrastive learning to improve intra-cluster consistency and inter-cluster discriminability.

During training, the SSCM starts with the use of K-means to generate pseudo-labels, and then PGM and SSCM forms a virtuous circle. In this circle, the former generates pseudo-labels to guide the latter in discovering sample similarity, while the similarity discovered by the latter in turn helps the former generate more reliable pseudo-labels. Meanwhile, the outputs from PGM are incorporated into CLM, assisting CLM in generating satisfactory clustering results.

3.2. Data Augmentation

Data augmentation is indispensable in contrastive learning. Consistent with previous studies, we utilize the *contextual augmenter* (Shorten et al., 2021) to generate augmented data, and its setting is the same as (Zheng et al., 2023; Zhang et al., 2021). Specifically, given a batch of N text samples, i.e., $\boldsymbol{X}^{(0)} = [\boldsymbol{x}_1^{(0)}; \ldots; \boldsymbol{x}_N^{(0)}]$, *contextual augmenter* generates augmented texts that are $X^{(1)}$ and $X^{(2)}$. After that, Encoder Φ maps the data into the feature space, obtaining $\boldsymbol{V}^{(0)}$, $\boldsymbol{V}^{(1)}$ and $\boldsymbol{V}^{(2)}$, all of which are in $\mathbb{R}^{N \times D_1}$.

3.3. Pseudo-label Generation Module

The Pseudo-label Generation Module aims to produce reliable pseudo-labels. To achieve this, we propose a novel OT formulation (AEOT), by solving the AEOT problem, we can generate pseudo-labels that simultaneously integrate sample-to-sample semantic consistency and sample-to-cluster global structural information.

The structure of the Pseudo-label Generation Module is shown in Figure 1(a). Given a batch of original text representations $\boldsymbol{V}^{(0)}$, we use a fully connected neural network G_p to predict probability assignments $\boldsymbol{P}^{(0)} = G_p(\boldsymbol{V}^{(0)}) \in \mathbb{R}^{N \times K}$, where K is the number of clusters. Then, pseudo-labels can be generated by solving AEOT problem as follows:

$$\begin{aligned} &\min_{\boldsymbol{Q},\boldsymbol{b}} \langle \boldsymbol{Q}, \boldsymbol{M} \rangle + \varepsilon_1 H(\boldsymbol{Q}) + \varepsilon_2 (\Psi(\boldsymbol{b})^T \mathbf{1}) - \varepsilon_3 \langle \boldsymbol{S}, \boldsymbol{Q}\boldsymbol{Q}^T \rangle \\ &\text{s.t.} \quad \boldsymbol{Q}\mathbf{1} = \boldsymbol{a},\ \boldsymbol{Q}^T\mathbf{1} = \boldsymbol{b},\ \boldsymbol{Q} \geq 0,\ \boldsymbol{b}^T\mathbf{1} = 1, \end{aligned} \tag{1}$$

where $\langle \cdot, \cdot \rangle$ represents the Frobenius inner product, ε_1, ε_2 and ε_3 are balancing hyperparameters, $\boldsymbol{S} = \boldsymbol{S}^{cos} + \boldsymbol{S}^{att}$ is the semantic similarity matrix, where $\boldsymbol{S}^{cos}$ is the cosine similarity matrix of the probability assignment $P^{(0)}$, and $\boldsymbol{S}^{att}$ is the attention similarity matrix generated from the attention network (G_h) by Eq. (6). The details of each term in Eq. (16) are as follows:

- $H(\boldsymbol{Q}) = \langle \boldsymbol{Q}, \log \boldsymbol{Q} - 1 \rangle$ is the entropy regularization term, which prevents the optimal transport solution from being sparse.
- $\Psi(\boldsymbol{b}) = -\log(\boldsymbol{b}) - \log(1 - \boldsymbol{b})$ is a penalty term applied to the cluster probabilities $\boldsymbol{b}$, which encourages $\boldsymbol{b}$ to approach a uniform distribution. By adjusting the strength of this term, AEOT can be applied to datasets with various levels of imbalance.

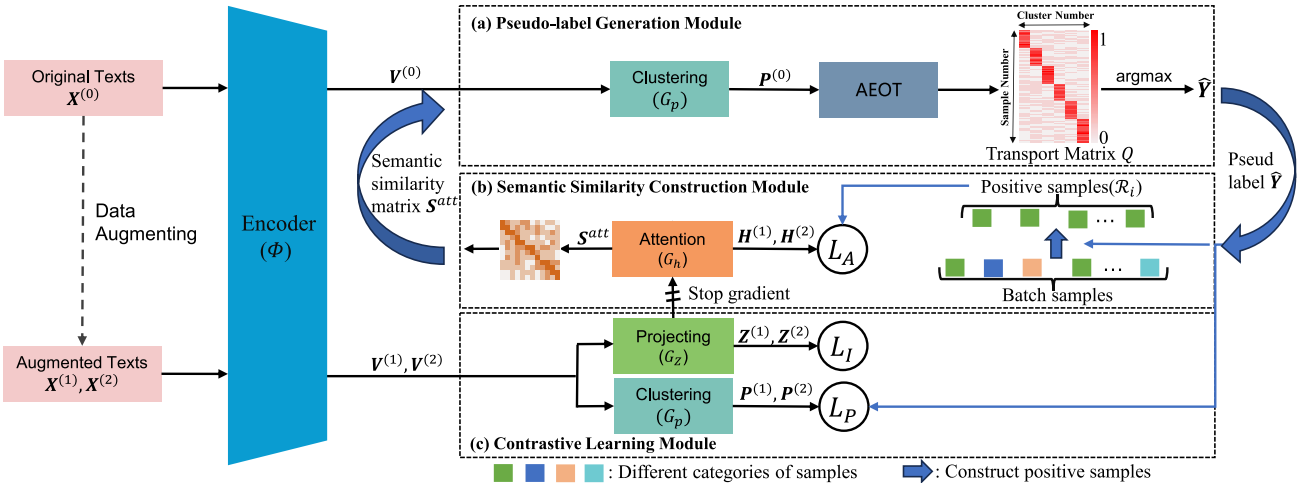

Figure 2: Overall structure of POTA. Our model contains three components: (a) Pseudo-label Generation Module, (b) Semantic Similarity Construction Module and (c) Contrastive Learning Module.

- $\langle \boldsymbol{S}, \boldsymbol{Q}\boldsymbol{Q}^T \rangle$ is the semantic regularization term, which encourages the transport matrix $\boldsymbol{Q}$ to maintain semantic consistency between samples. Specifically, this term encourages $\boldsymbol{Q}_{i:}$ to be similar to $\boldsymbol{Q}_{j:}$ if $\boldsymbol{S}_{ij}$ is large. In other words, this term encourages semantically similar samples to generate similar transport vectors, thereby producing reliable pseudo-labels.

Our proposed AEOT is a novel OT formulation with a complex quadratic semantic regularization term. It cannot be directly solved using conventional OT methods. To this end, inspired by CSOT we propose integrating Lagrange multiplier algorithm (Zheng et al., 2023) into the generalized conditional gradient (GCG) algorithm (Yu et al., 2017) to solve AEOT. The specific solution method is detailed in Appendix A.1.

After obtaining $\boldsymbol{Q}$, pseudo-labels can be generated by argmax operation as follows:

$$\hat{\boldsymbol{Y}}_{ij} = \begin{cases} 1, & \text{if } j = \arg\max_{j'} \boldsymbol{Q}_{ij'} \\ 0, & \text{otherwise} \end{cases} \tag{2}$$

In our proposed AEOT, the inherent global minimum-cost matching mechanism of optimal transport introduces sample-to-cluster global structure information into the transport matrix $\boldsymbol{Q}$, while the term $\langle \boldsymbol{S}, \boldsymbol{Q}\boldsymbol{Q}^T \rangle$ incorporates sample-to-sample semantic consistency into the transport matrix $\boldsymbol{Q}$, which helps us generate more accurate and reliable pseudo-labels $\hat{\boldsymbol{Y}}$.

3.4. Semantic Similarity Construction Module

Semantic Similarity Construction Module produces semantic similarities between samples. Inspired by (Liu et al., 2024; Vaswani et al., 2017), we use the attention mechanism at the instance level to explore their similarity relationships. The structure of the Attention network is shown in Figure 3. By mapping the augmented representations $\boldsymbol{V}^{(1)}$ and $\boldsymbol{V}^{(2)}$ via the Projecting network G_z (Fully Connected Neural Network), one obtains $\boldsymbol{Z}^{(1)}$ and $\boldsymbol{Z}^{(2)} \in \mathbb{R}^{N \times D_2}$, which in turn are used as the input to the Attention network G_h.

The output of the Attention network G_h consists of two augmented representations, namely $\boldsymbol{H}^{(1)}$ and $\boldsymbol{H}^{(2)}$. Specifically, taking $\boldsymbol{Z}^{(1)}$ as an example, it is firstly mapped to different feature spaces by $\boldsymbol{W}_{K_1}$, $\boldsymbol{W}_{K_2}$ and $\boldsymbol{W}_T$:

$$\boldsymbol{K}_1^{(1)} = \boldsymbol{Z}^{(1)}\boldsymbol{W}_{K_1}, \boldsymbol{K}_2^{(1)} = \boldsymbol{Z}^{(1)}\boldsymbol{W}_{K_2}, \boldsymbol{T}^{(1)} = \boldsymbol{Z}^{(1)}\boldsymbol{W}_T, \tag{3}$$

after which the similarity matrix $\boldsymbol{S}^{(1)}$ is computed as follows:

$$\boldsymbol{S}^{(1)} = \text{Softmax}\left(\frac{\boldsymbol{K}_1^{(1)}\boldsymbol{K}_2^{(1)T}}{\sqrt{D_2}}\right), \tag{4}$$

the rows in $\boldsymbol{T}^{(1)}$ are weighted summed to produce a new representation:

$$\boldsymbol{h}_i^{(1)} = \sum_{j=1}^{N} \boldsymbol{S}_{ij}^{(1)} \boldsymbol{t}_j^{(1)}, \quad \boldsymbol{H}^{(1)} = [\boldsymbol{h}_1^{(1)}; \boldsymbol{h}_2^{(1)}; \ldots; \boldsymbol{h}_N^{(1)}], \tag{5}$$

where $\boldsymbol{t}_j^{(1)}$ is the jth row of $\boldsymbol{T}^{(1)}$, and $\boldsymbol{S}_{ij}^{(1)}$ is the (i,j)th element in $\boldsymbol{S}^{(1)}$. In the same way, $\boldsymbol{S}^{(2)}$ and $\boldsymbol{H}^{(2)}$ are obtained by passing $\boldsymbol{Z}^{(2)}$ through the Attention network. In this paper, we define $\boldsymbol{H} = [\boldsymbol{H}^{(1)}, \boldsymbol{H}^{(2)}]$ as the consistent representation and compute the attention similarity matrix $\boldsymbol{S}^{att}$ as follows:

$$\boldsymbol{S}^{att} = \frac{1}{2}\left(\boldsymbol{S}^{(1)} + \boldsymbol{S}^{(2)}\right). \tag{6}$$

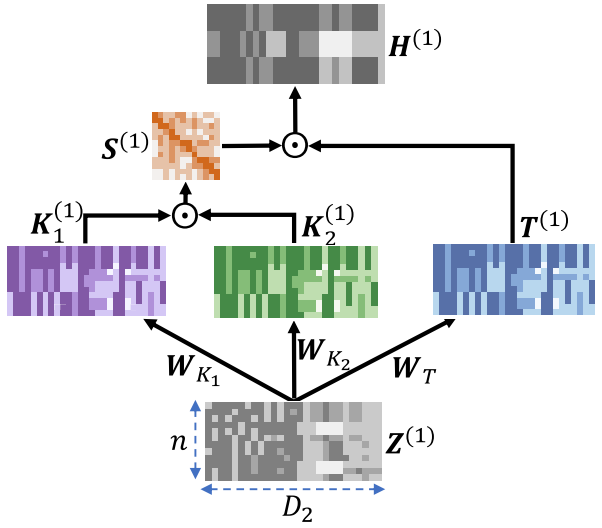

Figure 3: The structure of Attention network. $\boldsymbol{S}^{(1)}$ denotes the similarity matrix among samples.

According to Eq. (5), the attention similarity matrix $\boldsymbol{S}^{att}$ and the consistency representations $\boldsymbol{H}$ are interconnected. Inspired by this, we train the attention similarity matrix by enhancing the correlation among the consistency representations from the same cluster with the help of pseudo-labels. Specifically, we first use the pseudo-labels to determine samples in the same cluster. For the ith sample, the indices of samples in the same cluster are as follows:

$$\mathcal{R}_i = \{j \mid \hat{\boldsymbol{y}}_j = \hat{\boldsymbol{y}}_i, j = 1, ..., N\}, \tag{7}$$

where $\hat{\boldsymbol{y}}_i$ is the ith row of $\hat{\boldsymbol{Y}}$, which is the pseudo-label of the ith sample.

After that, the loss for the ith sample is defined as follows:

$$l_{A,i} = -\log \frac{\sum_{j\in\mathcal{R}_i} \boldsymbol{S}_{ij}^{att} [e^{\text{sim}(\boldsymbol{h}_i,\boldsymbol{h}_j)/\tau_A} + e^{\text{sim}(\boldsymbol{h}_i,\boldsymbol{h}_{N+j})/\tau_A}]}{\sum_{v=1,v\neq i}^{2N} e^{\text{sim}(\boldsymbol{h}_i,\boldsymbol{h}_v)/\tau_A}} - \log \frac{\sum_{j\in\mathcal{R}_i} \boldsymbol{S}_{ij}^{att} [e^{\text{sim}(\boldsymbol{h}_{N+i},\boldsymbol{h}_j)/\tau_A} + e^{\text{sim}(\boldsymbol{h}_{N+i},\boldsymbol{h}_{N+j})/\tau_A}]}{\sum_{v=1,v\neq i}^{2N} e^{\text{sim}(\boldsymbol{h}_{N+i},\boldsymbol{h}_v)/\tau_A}}, \tag{8}$$

where $\boldsymbol{S}_{ij}^{att}$ is the (i,j)th element in $\boldsymbol{S}^{att}$, $\boldsymbol{h}_i$ is the ith row of $\boldsymbol{H}$, τ_A is the temperature parameter, and $sim(\boldsymbol{h}_i, \boldsymbol{h}_j)$ is the cosine similarity between two samples defined as follows:

$$\text{sim}(\boldsymbol{h}_i, \boldsymbol{h}_j) = \frac{\langle \boldsymbol{h}_i, \boldsymbol{h}_j \rangle}{\|\boldsymbol{h}_i\| \, \|\boldsymbol{h}_j\|}. \tag{9}$$

The overall loss is the average of all the samples in the batch, which is defined as follows:

$$L_A = \frac{1}{2N} \sum_{i=1}^{N} l_{A,i}. \tag{10}$$

By minimizing L_A, sample cluster samples will receive higher weights in the attention similarity matrix $\boldsymbol{S}^{att}$, which are then used in PGM to facilitate optimal transport. It should be noted that we adopt the *stop gradient* technique during the backpropagation of the L_A loss, and this loss is solely used to optimize the Attention network.

3.5. Contrastive Learning Module

The Contrastive Learning Module simultaneously performs cluster-level and instance-level contrastive learning to learn discriminative representations and clustering. The structure of the Contrastive Learning Module is shown in Figure 2(c). Given a batch of text representations $\boldsymbol{V}^{(1)}$ and $\boldsymbol{V}^{(2)}$, one can obtain the projected representations $\boldsymbol{Z}^{(1)}$ and $\boldsymbol{Z}^{(2)}$, the probability assignments $\boldsymbol{P}^{(1)}$ and $\boldsymbol{P}^{(2)}$. Then, $\boldsymbol{Z}^{(1)}$, $\boldsymbol{Z}^{(2)}$, $\boldsymbol{P}^{(1)}$ and $\boldsymbol{P}^{(2)}$ are used in both cluster-level and instance-level contrastive learning.

The cluster-level contrastive learning utilizes pseudo-labels generated by the PGM as supervision to enhance intra-cluster cohesion and inter-cluster separation. Specifically, we use pseudo-labels as supervised information to identify the category of the samples, and then optimize the probability distributions of the same category samples to converge toward a single one-hot vector, while samples from different categories move toward distinct one-hot vectors. This process can be achieved using the cross-entropy loss function, shown as follows:

$$L_P = -\frac{1}{N} \sum_{i=1}^{N} (\hat{\boldsymbol{y}}_i \log \boldsymbol{p}_i^{(1)} + \hat{\boldsymbol{y}}_i \log \boldsymbol{p}_i^{(2)}), \tag{11}$$

where $\hat{\boldsymbol{y}}_i$ is the pseudo-label for the ith sample, $\boldsymbol{p}_i^{(1)}$ and $\boldsymbol{p}_i^{(2)}$ are the ith row of the augmented probability matrix $\boldsymbol{P}^{(1)}$ and $\boldsymbol{P}^{(2)}$, respectively.

The instance-level contrastive learning aims to learn representations by bringing positive pairs closer while pushing negative pairs apart. For the ith sample, its augmented samples are regarded as a positive pair $\left\{\boldsymbol{z}_i^{(1)}, \boldsymbol{z}_i^{(2)}\right\}$, while the other $2N-2$ pairs are considered negative. The loss function for the ith sample is defined as follows:

$$l_{I,i} = -\log \frac{e^{sim(\boldsymbol{z}_i^{(1)},\boldsymbol{z}_i^{(2)})/\tau_I}}{\sum_{k=1,k\neq i}^{N} (e^{sim(\boldsymbol{z}_i^{(1)},\boldsymbol{z}_k^{(1)})/\tau_I} + e^{sim(\boldsymbol{z}_i^{(1)},\boldsymbol{z}_k^{(2)})/\tau_I})} - \log \frac{e^{sim(\boldsymbol{z}_i^{(2)},\boldsymbol{z}_i^{(1)})/\tau_I}}{\sum_{k=1,k\neq i}^{N} (e^{sim(\boldsymbol{z}_i^{(2)},\boldsymbol{z}_k^{(1)})/\tau_I} + e^{sim(\boldsymbol{z}_i^{(2)},\boldsymbol{z}_k^{(2)})/\tau_I})}, \tag{12}$$

where τ_I is the temperature parameter. The instance-level contrastive loss is computed over all samples in the batch:

$$L_I = \frac{1}{2N} \sum_{i=1}^{N} l_{I,i}. \tag{13}$$

3.6. Putting Together

The overall learning procedure of POTA in Algorithm 1. Specifically, we first perform a warm-up stage. In this stage, pseudo-labels are generated by the K-means algorithm on original text representations $V^{(0)}$ instead of PGM. The Warm-up loss consists of L_I and L_A as follows:

$$L = L_A + \lambda L_I, \tag{14}$$

After the Warm-up stage, the semantic similarity matrix has been trained, it is then used to assist the PGM in generating pseudo-labels. The total loss at this stage is as follows:

$$L = L_A + L_P + \lambda L_I, \tag{15}$$

where λ is a balancing hyperparameter. After training, for a given text $\boldsymbol{x}^{(\mathbf{0})}$, its clustering result is calculated using $\text{argmax}(\boldsymbol{p}^{(0)})$.

Algorithm 1 POTA

Input: Dataset $\mathcal{X}^{(0)}$; number of warm-up epochs E_{warm}; number of total epochs E_{total}; batch size N.
Output: the clustering model.
Generate augmented dataset $\mathcal{X}^{(1)}$ and $\mathcal{X}^{(2)}$ based on $\mathcal{X}^{(0)}$.
Load the pre-trained SBERT as encoder Φ and initialize parameters in network G_z, G_h, and G_p.
for $epoch = 1$ **to** E_{total} **do**
  Sample a mini-batch $\left\{\boldsymbol{X}^{(0)}, \boldsymbol{X}^{(1)}, \boldsymbol{X}^{(2)}\right\}$.
  Compute representations $\boldsymbol{V}^{(0)}, \left\{\boldsymbol{Z}^{(1)}, \boldsymbol{Z}^{(2)}\right\}, \left\{\boldsymbol{H}^{(1)}, \boldsymbol{H}^{(2)}\right\}$ and probability assignments $\left\{\boldsymbol{P}^{(1)}, \boldsymbol{P}^{(2)}\right\}$.
  if $epoch \leq E_{warm}$ **then**
    Compute pseudo-labels $\hat{Y}$ by k-means.
    Construct the set $\mathcal{R}$ based on $\hat{Y}$ in Eq. (7).
    Compute the loss $L = L_A + \lambda L_I$ in Eq. (14).
    Update parameters in Φ, G_z and G_h.
  else
    Compute probability assignments $\boldsymbol{P}^{(0)}$.
    Compute pseudo-labels $\hat{Y}$ by AEOT.
    Construct the set $\mathcal{R}$ based on $\hat{Y}$ in Eq. (7).
    Compute loss $L = L_A + L_P + \lambda L_I$ in Eq. (15).
    Update parameters in Φ, G_z, G_h, and G_p.
  end if
end for

4. Experiments

4.1. Datasets

We experimented with eight benchmark datasets: **AgNews**, **StackOverflow**, **Biomedical**, **SearchSnippets**, **GoogleNews-TS**, **GoogleNews-T**, **GoogleNews-S** and **Tweet**. Table 1 summarizes the datasets' information. According to the imbalance degree, **AgNews**, **StackOverflow** and **Biomedical** are regarded as balanced datasets, **SearchSnippets** is a slightly imbalanced dataset, **GoogleNews-TS**, **GoogleNews-T** and **GoogleNews-S** are imbalanced datasets, **Tweet** is a severely imbalanced dataset.

Datasets	S	N	L	R
AgNews	8000	4	23	1
SearchSnippets	12340	8	18	7
StackOverflow	20000	20	8	1
Biomedical	20000	20	13	1
GoogleNews-TS	11109	152	8	143
GoogleNews-T	11109	152	6	143
GoogleNews-S	11109	152	22	143
Tweet	2472	89	22	249

Table 1: Key information of datasets. "S" represent the dataset size; "N" is the number of categories; "L" is the average sentence length; "R" is the size ratio of the largest to the smallest category.

4.2. Experiment Settings

We use the distilbert-base-nli-stsb-mean-tokens (SBERT) in the Sentence Transformers library as Encoder(Reimers & Gurevych, 2019). All parameters of our model are optimized using the Adam optimizer, and the learning rate of the Encoder is 5×10^{-6}, while the learning rate of other networks is 5×10^{-4}. We set $\varepsilon_1 = 1$, $\varepsilon_3 = 25$ and $\lambda = 10$ for all datasets, $\varepsilon_2 = 100$, 3.5, 0.06 and 0.03 for balanced, slightly imbalanced, imbalanced and severely imbalanced datasets, respectively. We adopt Accuracy (ACC) and Normalized Mutual Information (NMI) to evaluate model. The definitions of the evaluation methods and other settings are provided in Appendix B.2 and Appendix B.3, respectively.

4.3. Baselines

We compare our method with several short text clustering approaches. **BOW** (Scott & Matwin, 1998) and **TF-IDF** (Chowdhury, 2010) utilize the BOW and TF-IDF techniques to extract text data representations, respectively, and employ k-means for clustering. **Self-Train** (Hadifar et al., 2019) uses an auto-encoder to learn representations and updates parameters according to cluster assignments. **SCCL** (Zhang et al., 2021) employs contrastive learning to refine the output of SBERT as representations and obtains the clustering results using the DEC algorithm (Xie et al., 2016). **RSTC** (Zheng et al., 2023) constructs pseudo-labels using optimal transport to assist the model in training neural networks for clustering. Additionally, we include the **SBERT** experiment, which applies k-means directly to the output of SBERT, it is the initial state of our model.

	AgNews		SearchSnippets		Stackoverflow		Biomedical	
	ACC	NMI	ACC	NMI	ACC	NMI	ACC	NMI
BOW	28.71	4.07	23.67	9.00	17.92	13.21	14.18	8.51
TF-IDF	34.39	12.19	30.85	18.67	58.52	59.02	29.13	25.12
Self-Train	-	-	72.69	56.74	59.38	52.81	40.06	34.46
SCCL	83.10	61.96	79.90	63.78	70.83	69.21	42.49	**39.16**
RSTC	85.99	64.14	79.83	**68.76**	80.07	72.28	45.69	38.57
SBERT	64.40	30.69	54.47	30.48	60.50	51.72	38.30	32.19
POTA	**87.30**	**66.55**	**80.12**	67.40	**85.96**	**75.43**	**47.37**	39.12
Improvement	**+1.31**	**+2.41**	**+0.29**	**-1.36**	**+5.89**	**+3.15**	**+1.68**	**-0.04**
	GoogleNews-TS		**GoogleNews-T**		**GoogleNews-S**		**Tweet**	
	ACC	NMI	ACC	NMI	ACC	NMI	ACC	NMI
BOW	58.79	82.59	48.05	72.38	52.68	76.11	50.25	72.00
TF-IDF	69.00	87.78	58.36	79.14	62.30	83.00	54.34	78.47
SCCL	82.51	93.01	69.01	85.10	73.44	87.98	73.10	86.66
RSTC	83.30	92.62	73.10	87.47	78.11	89.01	77.75	86.07
SBERT	65.49	86.39	59.75	79.54	59.54	80.65	53.80	79.05
POTA	**83.53**	**93.15**	**73.47**	**87.54**	**79.57**	**89.3**	**82.36**	**89.49**
Improvement	**+0.23**	**+0.53**	**+0.37**	**+0.07**	**+1.46**	**+0.29**	**+4.61**	**+3.42**

Table 2: Experimental results on eight short text datasets. Bold fonts represent the best results.

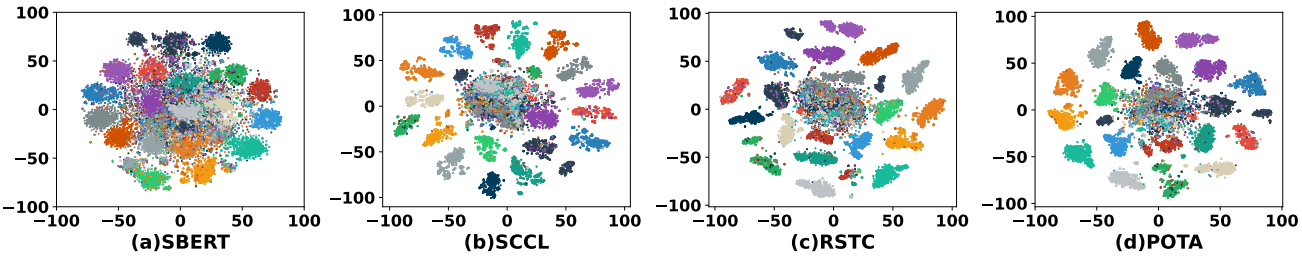

Figure 4: T-SNE visualization of the representations on Stackoverflow, each color indicates ground truth category.

4.4. Performance and Analysis

The results on eight benchmark datasets are shown in Table 2. Note that the results of RSTC were reproduced using the configuration provided by the authors, while the remaining baseline results are derived from the reported in the RSTC paper. According to the results, we can conclude that: (1) Conventional methods (**BOW** and **TF-IDF**) perform poorly due to their inability to produce meaningful representations. (2) Deep neural network-based methods (**STCC** and **Self-Train**) are more effective than conventional methods in learning efficient representations. However, their decoupled feature extraction and clustering processes result in suboptimal outcomes. (3) **SCCL** and **RSTC** highly improved the cluster performance by using contrastive learning to fine-tune pre-trained models. However, they ignored the relationships between samples, which led to negative effects. (4) our proposed **POTA** achieves best results on six datasets and matches results on **SearchSnippets** and **GoogleNews-T**. Besides, our method makes substantial improvements on **Stackoverflow** and **Tweet** datasets. The superb results demonstrate the effectiveness of our method.

Furthermore, we performed T-SNE visualization of representations in previous works and our method. The result is shown in Figure 4. We can see that: (1) in **SBERT**, all the clusters overlap with each other. (2) **SCCL** shows partial improvement than SBERT, with some clusters forming effectively. However, the points within these clusters are dispersed, indicating lower intra-cluster cohesion. (3) **RSTC** achieves higher intra-cluster cohesion than SCCL, demonstrating that pseudo-labels effectively aid the model in learning discriminative representations. (4) Our proposed **POTA** achieves the best clustering performance. It effectively reduces the noise points within the clusters obtained by clustering. The representation visualization indicates that

our proposed method learned discriminative representations and achieved better clustering.

4.5. Comparison of representation quality

To demonstrate that our model actually produces more discriminative representations, we conducted a comparative study with SCCL and RSTC on the **SearchSnippets** and **GoogleNews-TS** datasets. We used the average cosine similarity of sample representations within the same class as the evaluation metric, where the "same class" was defined based on their ground-truth labels.

The results are presented in Figure 5. From these results, we can find that: (1) RSTC achieves higher representation quality compared to SCCL, demonstrating that leveraging pseudo-labels to guide the learning of more meaningful representations is effective. (2) Our method significantly surpasses both SCCL and RSTC by a large margin, demonstrating its superior capacity to learn robust and discriminative representations. These results clearly highlight the effectiveness of our approach in improving the representation quality.

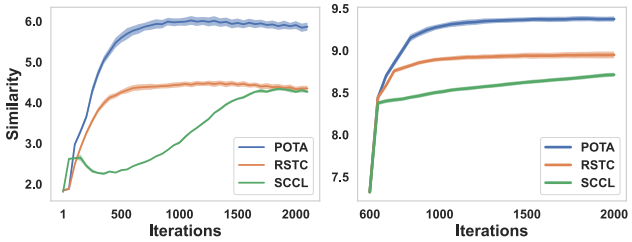

(a) StackOverflow (b) GoogleNews-TS

Figure 5: The comparison of representation quality. The shaded regions represent the variance derived from 50 runs with different random seeds.

4.6. Ablation Study

In this section, we conduct an ablation study to validate the effectiveness of semantic regularization in AEOT. To be specific, in our proposed AEOT in Eq. (1), the semantic regularization term $\langle \boldsymbol{S}, \boldsymbol{Q}\boldsymbol{Q}^T \rangle$ plays a crucial role, as it simultaneously used the attention similarity matrix $\boldsymbol{S}^{att}$ and the cosine similarity matrix $\boldsymbol{S}^{cos}$. To demonstrate the significance of semantic regularization, we performed ablation studies by removing one or both of these similarity matrices, i.e. **No Cos**, **No Att** and **No All**.

The results in Table 3, the comparison between **POTA** and **No All** demonstrates that semantic regularization is indispensable. The comparison between **POTA** with **No Att** and **No Cos** shows that our method outperforms using a single similarity matrix, This is because exploring similarities in different spaces allows for a comprehensive understanding of the semantic relationships between samples. Finally, the comparison between **No Att** and **No Cos** indicates that our proposed attention mechanism is more effective than previous methods that use cosine similarity to capture semantic similarity relationships.

Datasets	Method	ACC	NMI
SearchSnippets	POTA	**80.12**	**67.40**
	No Cos	78.81	66.14
	No Att	76.86	65.93
	No All	78.93	66.21
StackOverflow	POTA	**85.96**	**75.43**
	No Cos	83.52	73.89
	No Att	79.11	70.89
	No All	80.31	72.45
GoogleNews-TS	POTA	**83.53**	**93.15**
	No Cos	81.83	92.68
	No Att	80.34	91.03
	No All	81.27	91.18

Table 3: Effectiveness of semantic regularization in AEOT.

4.7. Case Study

In addition to the experiments mentioned above, we conducted several additional experiments to further explore the capabilities of POTA. To evaluate the effectiveness of our proposed OT formulation for generating pseudo-labels, we compared it with other popular pseudo-labeling methods. The results are detailed in Appendix C. Additionally, we performed ablation experiments to assess the significance of cluster-level and instance-level contrastive learning, with the corresponding results presented in Appendix C.1. Our model involves several hyperparameters, including ε_1, ε_2, ε_3, and λ. The experimental results and analysis related to these hyperparameters are provided in Appendix D.

5. Conclusion

In this paper, our proposed POTA framework effectively enhances the performance of short text clustering by generating highly discriminative representations. By leveraging an attention mechanism to capture sample semantic relationships and utilizing semantic-aware adaptive optimal transport, POTA produces reliable pseudo-labels that consider both sample-to-cluster global structure and sample-to-sample semantic relationships. Then, we use pseudo-labels to guide contrastive learning to learn more discriminative representations, significantly enhancing clustering efficiency and accuracy. Extensive experiments on eight benchmark datasets confirm the effectiveness of POTA.

References

Ahmed, M. H., Tiun, S., Omar, N., and Sani, N. S. Short text clustering algorithms, application and challenges: A survey. *Applied Sciences*, 13(1):342, 2022.

Asano, Y. M., Rupprecht, C., and Vedaldi, A. Self-labelling via simultaneous clustering and representation learning. In *International Conference on Learning Representations (ICLR)*, 2020.

Berthelot, D., Carlini, N., Cubuk, E. D., Kurakin, A., Sohn, K., Zhang, H., and Raffel, C. Remixmatch: Semi-supervised learning with distribution matching and augmentation anchoring. In *International Conference on Learning Representations*, 2020.

Bertsekas, D. P. *Constrained optimization and Lagrange multiplier methods*. Academic press, 2014.

Caron, M., Misra, I., Mairal, J., Goyal, P., Bojanowski, P., and Joulin, A. Unsupervised learning of visual features by contrasting cluster assignments. *Advances in neural information processing systems*, 33:9912–9924, 2020.

Chang, W., Shi, Y., and Wang, J. Csot: Curriculum and structure-aware optimal transport for learning with noisy labels. *Advances in Neural Information Processing Systems*, 36:8528–8541, 2023.

Chowdhury, G. G. *Introduction to modern information retrieval*. Facet publishing, 2010.

Gupta, D., Ramjee, R., Kwatra, N., and Sivathanu, M. Unsupervised clustering using pseudo-semi-supervised learning. In *International Conference on Learning Representations*, 2020.

Hadifar, A., Sterckx, L., Demeester, T., and Develder, C. A self-training approach for short text clustering. In *Proceedings of the 4th Workshop on Representation Learning for NLP (RepL4NLP-2019)*, pp. 194–199, 2019.

Huang, L., Shi, P., Zhu, H., and Chen, T. Early detection of emergency events from social media: A new text clustering approach. *Natural Hazards*, 111(1):851–875, 2022.

Liu, S., Liu, J., Yuan, H., Li, Q., Geng, J., Yuan, Z., and Han, H. Deep contrastive multi-view clustering under semantic feature guidance. *arXiv preprint arXiv:2403.05768*, 2024.

Papadimitriou, C. H. and Steiglitz, K. *Combinatorial optimization: algorithms and complexity*. Courier Corporation, 1998.

Peyré, G., Cuturi, M., et al. Computational optimal transport: With applications to data science. *Foundations and Trends® in Machine Learning*, 11(5-6):355–607, 2019.

Phan, X.-H., Nguyen, L.-M., and Horiguchi, S. Learning to classify short and sparse text & web with hidden topics from large-scale data collections. In *Proceedings of the 17th international conference on World Wide Web*, pp. 91–100, 2008.

Rakib, M. R. H., Zeh, N., Jankowska, M., and Milios, E. Enhancement of short text clustering by iterative classification. In *Natural Language Processing and Information Systems: 25th International Conference on Applications of Natural Language to Information Systems, NLDB 2020, Saarbrücken, Germany, June 24–26, 2020, Proceedings 25*, pp. 105–117. Springer, 2020.

Reimers, N. and Gurevych, I. Sentence-BERT: Sentence embeddings using Siamese BERT-networks. In *Proceedings of the 2019 Conference on Empirical Methods in Natural Language Processing and the 9th International Joint Conference on Natural Language Processing (EMNLP-IJCNLP)*, November 2019.

Scott, S. and Matwin, S. Text classification using wordnet hypernyms. In *Usage of WordNet in natural language processing systems*, 1998.

Shorten, C., Khoshgoftaar, T. M., and Furht, B. Text data augmentation for deep learning. *Journal of big Data*, 8 (1):101, 2021.

Shum, H.-Y., He, X.-d., and Li, D. From eliza to xiaoice: challenges and opportunities with social chatbots. *Frontiers of Information Technology & Electronic Engineering*, 19:10–26, 2018.

Sohn, K., Berthelot, D., Carlini, N., Zhang, Z., Zhang, H., Raffel, C. A., Cubuk, E. D., Kurakin, A., and Li, C.-L. Fixmatch: Simplifying semi-supervised learning with consistency and confidence. *Advances in neural information processing systems*, 33:596–608, 2020.

Taherdoost, H. Enhancing social media platforms with machine learning algorithms and neural networks. *Algorithms*, 16(6):271, 2023.

Vaswani, A., Shazeer, N., Parmar, N., Uszkoreit, J., Jones, L., Gomez, A. N., Kaiser, Ł., and Polosukhin, I. Attention is all you need. *Advances in neural information processing systems*, 30, 2017.

Xia, J., Tan, C., Wu, L., Xu, Y., and Li, S. Z. Ot cleaner: Label correction as optimal transport. In *ICASSP 2022-2022 IEEE International Conference on Acoustics, Speech and Signal Processing (ICASSP)*, pp. 3953–3957. IEEE, 2022.

Xie, J., Girshick, R., and Farhadi, A. Unsupervised deep embedding for clustering analysis. In *International conference on machine learning*, pp. 478–487. PMLR, 2016.

Xu, J., Xu, B., Wang, P., Zheng, S., Tian, G., and Zhao, J. Self-taught convolutional neural networks for short text clustering. *Neural Networks*, 88:22–31, 2017.

Yin, J. and Wang, J. A model-based approach for text clustering with outlier detection. In *2016 IEEE 32nd International Conference on Data Engineering (ICDE)*, pp. 625–636. IEEE, 2016.

Yu, Y., Zhang, X., and Schuurmans, D. Generalized conditional gradient for sparse estimation. *Journal of Machine Learning Research*, 18(144):1–46, 2017.

Zhang, C., Ren, H., and He, X. P2OT: progressive partial optimal transport for deep imbalanced clustering. In *The Twelfth International Conference on Learning Representations, ICLR 2024, Vienna, Austria, May 7-11, 2024*. OpenReview.net, 2024.

Zhang, D., Nan, F., Wei, X., Li, S.-W., Zhu, H., McKeown, K., Nallapati, R., Arnold, A. O., and Xiang, B. Supporting clustering with contrastive learning. In *North American Chapter of the Association for Computational Linguistics*, 2021.

Zhang, X., Zhao, J., and LeCun, Y. Character-level convolutional networks for text classification. *Advances in neural information processing systems*, 28, 2015.

Zheng, X., Hu, M., Liu, W., Chen, C., and Liao, X. Robust representation learning with reliable pseudo-labels generation via self-adaptive optimal transport for short text clustering. In *Annual Meeting of the Association for Computational Linguistics*, 2023.

A. Hyper-efficient Solution for AEOT

A.1. Formulation of the Solution

As mentioned in Section 3.3, the AEOT problem is formulated as:

$$\begin{aligned} &\min_{\boldsymbol{Q},\boldsymbol{b}} \langle \boldsymbol{Q}, -\log\left(\boldsymbol{P}^{(0)}\right)\rangle + \varepsilon_1 H(\boldsymbol{Q}) + \varepsilon_2(\Psi(\boldsymbol{b})^T\mathbf{1}) - \varepsilon_3\langle \boldsymbol{S}, \boldsymbol{Q}\boldsymbol{Q}^T\rangle \\ &\text{s.t.} \quad \boldsymbol{Q}\mathbf{1} = \boldsymbol{a},\ \boldsymbol{Q}^T\mathbf{1} = \boldsymbol{b},\ \boldsymbol{Q} \geq 0,\ \boldsymbol{b}^T\mathbf{1} = 1, \end{aligned} \tag{16}$$

where $\langle \cdot, \cdot \rangle$ represents the Frobenius inner product, ε_1 and ε_2 are balancing hyperparameters, $H(\boldsymbol{Q}) = \langle \boldsymbol{Q}, \log(\boldsymbol{Q}) - 1\rangle$ is the entropy regularization term, and $\Psi(\boldsymbol{b}) = -\log(\boldsymbol{b}) - \log(1 - \boldsymbol{b})$ is a penalty term on the cluster probabilities $\boldsymbol{b}$.

Our proposed AEOT with a complex quadratic semantic regularization term, which cannot be directly solved using conventional OT methods. To this end, inspired by CSOT (Chang et al., 2023), we propose a hyper-efficient solver that integrates Lagrange multiplier algorithm (Zheng et al., 2023) into the generalized conditional gradient (GCG) algorithm (Yu et al., 2017) to solve AEOT. Specifically, we first utilize the GCG algorithm linearize the complex quadratic term $\langle \boldsymbol{S}, \boldsymbol{Q}\boldsymbol{Q}^T\rangle$, then we employ the Lagrange multiplier algorithm to solve it.

To better explain the linearization of the semantic constraint term $\langle \boldsymbol{S}, \boldsymbol{Q}\boldsymbol{Q}^T\rangle$, we first define:

$$f(\boldsymbol{Q}) = \langle \boldsymbol{Q}, -\log(\boldsymbol{P}^{(0)})\rangle - \varepsilon_3\langle \boldsymbol{S}, \boldsymbol{Q}\boldsymbol{Q}^T\rangle, \tag{17}$$

the algorithm GCG is an iterative optimization algorithm. For the *i*th iteration, given the previously computed transport matrix $\boldsymbol{Q}_{i-1}$, the objective function $f(\boldsymbol{Q})$ is expanded using a Taylor series and only retained the linear term:

$$f_{\text{lin}}(\boldsymbol{Q}) = f(\boldsymbol{Q}_{i-1}) + \langle f'(\boldsymbol{Q}_{i-1}), \boldsymbol{Q} - \boldsymbol{Q}_{i-1}\rangle = \langle \boldsymbol{Q}, f'(\boldsymbol{Q}_{i-1})\rangle + f(\boldsymbol{Q}_{i-1}) - \langle \boldsymbol{Q}_{i-1}, f'(\boldsymbol{Q}_{i-1})\rangle, \tag{18}$$

since $\boldsymbol{Q}_{i-1}$ has already been computed, the term $f(\boldsymbol{Q}_{i-1}) - \langle \boldsymbol{Q}_{i-1}, f'(\boldsymbol{Q}_{i-1})\rangle$ is a constant, we use the letter C to represent it. Therefore, the Eq.(17) can be approximate to:

$$\begin{aligned} f(\boldsymbol{Q}) &\approx f_{\text{lin}}(\boldsymbol{Q}) \\ &= \langle \boldsymbol{Q}, f'(\boldsymbol{Q}_{i-1})\rangle + f(\boldsymbol{Q}_{i-1}) - \langle \boldsymbol{Q}_{i-1}, f'(\boldsymbol{Q}_{i-1})\rangle \\ &= \langle \boldsymbol{Q}, f'(\boldsymbol{Q}_{i-1})\rangle + C. \end{aligned} \tag{19}$$

Substituting Eq.(19) into Eq.(16), the AEOT problem can be approximately simplified as:

$$\begin{aligned} \min_{\boldsymbol{Q},\boldsymbol{b}} \quad & \langle \boldsymbol{Q}, f'(\boldsymbol{Q}_{i-1})\rangle + \varepsilon_1 H(\boldsymbol{Q}) + \varepsilon_2(\Psi(\boldsymbol{b})^T\mathbf{1}) \\ \text{s.t.} \quad & \boldsymbol{Q}\mathbf{1} = \boldsymbol{a}, \boldsymbol{Q}^T\mathbf{1} = \boldsymbol{b}, \boldsymbol{Q} \geq 0, \boldsymbol{b}^T\mathbf{1} = 1, \end{aligned} \tag{20}$$

where the formulation of $f'(\boldsymbol{Q}_{i-1})$ is provided in Appendix A.2. The pseudo-code of the GCG algorithm is presented in Algorithm 2.

Algorithm 2 Generalized Conditional Gradient Algorithm for AEOT with Quadratic Constraints

Input: Probability matrix $\boldsymbol{P}^{(0)}$; marginal constraints $\boldsymbol{a}$; semantic similarity matrix $\boldsymbol{S}$; constraints weights ε_1, ε_2 and ε_3.
Output: Transport matrix $\boldsymbol{Q}$.
Initialize $\boldsymbol{b}_0$ randomly and perform normalization so that $\boldsymbol{b}_0^T\mathbf{1} = 1$
Initialize $\boldsymbol{Q}_0 = \boldsymbol{a}\boldsymbol{b}_0^T$.
for i=1 to T_1 **do**
  $f'(\boldsymbol{Q}_{i-1}) = -\log(\boldsymbol{P}^{(0)}) - \varepsilon_3(\boldsymbol{S} + \boldsymbol{S}^T)\boldsymbol{Q}_{i-1}$.
  $\tilde{\boldsymbol{Q}}_i, \boldsymbol{b}_i = \arg\min_{\boldsymbol{Q},\boldsymbol{b}} \langle \boldsymbol{Q}, f'(\boldsymbol{Q}_{i-1})\rangle + \varepsilon_1 H(\boldsymbol{Q}) + \varepsilon_2(\Psi(\boldsymbol{b}_{i-1})^T\mathbf{1})$.
  Choose $\alpha_i \in [0, 1]$ so that it satisfies the Armijo rule.
  $\boldsymbol{Q}_i = (1 - \alpha_i)\boldsymbol{Q}_{i-1} + \alpha_i\tilde{\boldsymbol{Q}}_i$.
end for

Then, we adopt the Lagrangian multiplier algorithm to solve Eq.(20). For simplicity, we define $\boldsymbol{M}' = f'(\boldsymbol{Q}_{i-1})$:

$$\min_{\boldsymbol{Q},\boldsymbol{b}} \quad \langle \boldsymbol{Q}, \boldsymbol{M}' \rangle + \varepsilon_1 H(\boldsymbol{Q}) + \varepsilon_2(\Psi(\boldsymbol{b})^T\mathbf{1}) - \boldsymbol{f}^T(\boldsymbol{Q}\mathbf{1} - \boldsymbol{a}) - \boldsymbol{g}^T(\boldsymbol{Q}^T\mathbf{1} - \boldsymbol{b}) - h(\boldsymbol{b}^T\mathbf{1} - 1), \tag{21}$$

where $\boldsymbol{f}$, $\boldsymbol{g}$ and h are all Lagrangian multipliers. Taking the partial derivative of Eq.(21) with respect to $\boldsymbol{Q}$, we can obtain:

$$\boldsymbol{Q}_{ij} = \exp(\frac{\boldsymbol{f}_i + \boldsymbol{g}_j - \boldsymbol{M}'_{ij}}{\varepsilon_1}) > 0. \tag{22}$$

Eq.(22) is a function of $\boldsymbol{f}_i$ and $\boldsymbol{g}_j$. Next, we first fix $\boldsymbol{b}$, and update $\boldsymbol{f}_i$ and $\boldsymbol{g}_j$. Duo to the fact that $\boldsymbol{Q}\mathbf{1} = \boldsymbol{a}$, we can get:

$$\sum_{j=1}^{K} \boldsymbol{Q}_{ij} = \sum_{j=1}^{K} \exp(\frac{\boldsymbol{f}_i + \boldsymbol{g}_j - \boldsymbol{M}'_{ij}}{\varepsilon_1}) = \exp(\frac{\boldsymbol{f}_i}{\varepsilon_1}) \sum_{j=1}^{K} \exp(\frac{\boldsymbol{g}_j - \boldsymbol{M}'_{ij}}{\varepsilon_1}) = \boldsymbol{a}_i, \tag{23}$$

where K represents the number of classes in the dataset. Further, we can obtain:

$$\exp(\frac{\boldsymbol{f}_i}{\varepsilon_1}) = \frac{\boldsymbol{a}_i}{\sum_{j=1}^{K} \exp(\frac{\boldsymbol{g}_j - \boldsymbol{M}'_{ij}}{\varepsilon_1})}. \tag{24}$$

Taking the logarithm of both sides and multiplying by ε_1, we can obtain:

$$\boldsymbol{f}_i = \varepsilon_1 \ln \boldsymbol{a}_i - \varepsilon_1 \ln \sum_{j=1}^{K} \exp(\frac{\boldsymbol{g}_j - \boldsymbol{M}'_{ij}}{\varepsilon_1}). \tag{25}$$

Similar to the above derivation, duo to the fact that $\boldsymbol{Q}^T\mathbf{1} = \boldsymbol{b}$, we can obtain:

$$\boldsymbol{g}_j = \varepsilon_1 \ln \boldsymbol{b}_j - \varepsilon_1 \ln \sum_{i=1}^{N} \exp(\frac{\boldsymbol{f}_i - \boldsymbol{M}'_{ij}}{\varepsilon_1}). \tag{26}$$

We can observe that $\boldsymbol{g}_j$ is an unknown variable in Eq.(25), while $\boldsymbol{f}_i$ is an unknown variable in Eq.(26). Since $\boldsymbol{f}_i$ and $\boldsymbol{g}_j$ are functions of each other, making it infeasible to directly solve for their exact values. Thus, we employ an iterative approach to update and work out it.

Then, we fix $\boldsymbol{f}$ and $\boldsymbol{g}$, and update $\boldsymbol{b}$. Specifically, take the partial derivative of the optimization problem Eq.(21) on the variable $\boldsymbol{b}$, we can obtain:

$$(\boldsymbol{g}_j - h)\boldsymbol{b}_j^{(2)} - (\boldsymbol{g}_j - h + 2\varepsilon_2)\boldsymbol{b}_j + \varepsilon_2 = 0, \tag{27}$$

it is obvious that $\Delta_j = (\boldsymbol{g}_j - h)^{(2)} + 4\varepsilon_2^{(2)} > 0$. Thus, the Eq.(27) has a feasible solution:

$$\boldsymbol{b}_j(h) = \frac{(\boldsymbol{g}_j - h + 2\varepsilon_2) \pm \sqrt{\Delta_j}}{2(\boldsymbol{g}_j - h)}, \tag{28}$$

it can be easily proven that when the numerator is taken as '+', $\boldsymbol{b}_j(h) \geq 1$, which leads to an error in $\Psi(\boldsymbol{b}) = -\log(\boldsymbol{b}) - \log(1 - \boldsymbol{b})$. Therefore, the formulation of $\boldsymbol{b}_j(h)$ as follow:

$$\boldsymbol{b}_j(h) = \frac{(\boldsymbol{g}_j - h + 2\varepsilon_2) - \sqrt{\Delta_j}}{2(\boldsymbol{g}_j - h)}. \tag{29}$$

Taking Eq.(29) back to the original constraint $\boldsymbol{b}^T\mathbf{1} = 1$, the formula is defined as below:

$$(\boldsymbol{b}(\boldsymbol{h}))^T\mathbf{1} = 1, \tag{30}$$

where h is the root of Eq.(30), and we use Newton's method to work out it, the iteration of the Newton's method is set to be 10. Then, we can obtain $\boldsymbol{b}$ by Eq.(29).

Overall, through iteratively updating the Eq.(25), (26), (29), and (30), we can get the transport matrix $\boldsymbol{Q}$ on Eq.(22). We demonstrate the iterative optimization process for solving Eq.(20) using the Lagrange multiplier algorithm in Algorithm 3.

Algorithm 3 The optimization scheme of AEOT

Input: The cost distance matrix $\boldsymbol{M}'$; cluster probability b;
Output: The transport matrix $\boldsymbol{Q}$
Procedure:
Initialize $\boldsymbol{f}$ and $\boldsymbol{g}$ randomly.
Initialize $h = 1$.
for i=1 to T_2 **do**
Fix $\boldsymbol{b}$, update $\boldsymbol{f}$ and $\boldsymbol{g}$ by Eq.(25) and Eq.(26), respectively.
Fix $\boldsymbol{f}$ and $\boldsymbol{g}$, update $\boldsymbol{b}$ by Eq.(29) and Eq.(30).
end for
Calculate $\boldsymbol{Q}$ in Eq.(22).

A.2. Derivative Complement

The calculation of $f'(\boldsymbol{Q}_{i-1})$ in E.q.(20) is as follows:

$$\begin{aligned}\frac{\partial f(\boldsymbol{Q}_{i-1})}{\partial \boldsymbol{Q}} &= \frac{\partial \langle \boldsymbol{Q}, -\log(\boldsymbol{P}^{(0)})\rangle - \varepsilon_3 \langle \boldsymbol{S}, \boldsymbol{Q}\boldsymbol{Q}^T\rangle}{\partial \boldsymbol{Q}} \\ &= -\log(\boldsymbol{P}^{(0)}) - \varepsilon_3 \frac{\partial \langle \boldsymbol{S}, \boldsymbol{Q}\boldsymbol{Q}^T\rangle}{\partial \boldsymbol{Q}},\end{aligned} \tag{31}$$

where:

$$\begin{aligned}\frac{\partial \langle \boldsymbol{S}, \boldsymbol{Q}\boldsymbol{Q}^T\rangle}{\partial \boldsymbol{Q}} &= \frac{\partial \mathrm{tr}(\boldsymbol{S}^T\boldsymbol{Q}\boldsymbol{Q}^T)}{\partial \boldsymbol{Q}} = \frac{\partial \mathrm{tr}((\boldsymbol{S}^T\boldsymbol{Q}\boldsymbol{Q}^T)^T)}{\partial \boldsymbol{Q}} \\ &= \frac{\partial \mathrm{tr}(\boldsymbol{Q}\boldsymbol{Q}^T\boldsymbol{S})}{\partial \boldsymbol{Q}} = \frac{\partial \mathrm{tr}(\boldsymbol{Q}^T\boldsymbol{S}\boldsymbol{Q})}{\partial \boldsymbol{Q}} \\ &= (\boldsymbol{S} + \boldsymbol{S}^T)\boldsymbol{Q},\end{aligned} \tag{32}$$

therefore, the final computation result is as follows:

$$\frac{\partial f(\boldsymbol{Q}_{i-1})}{\partial Q} = -\log(\boldsymbol{P}^{(0)}) - \varepsilon_3(\boldsymbol{S} + \boldsymbol{S}^T)\boldsymbol{Q}. \tag{33}$$

B. Experiment

B.1. Datasets

We evaluated our POTA model using eight established datasets specifically curated for short-text clustering analysis. These datasets represent diverse text sources ranging from news headlines to social media posts, allowing for comprehensive model assessment across different domains. Table 4 summarizes key information about these datasets. Brief descriptions of these datasets are provided as follows:

- **AgNews** drawn from AG's news corpus (Zhang et al., 2015), contains 8,000 news headlines categorized into four topics (Rakib et al., 2020).
- **SearchSnippets** is extracted from web search transactions. It consists of 12,340 web search results classified into eight categories (Phan et al., 2008).
- **StackOverflow** consists of 20,000 question titles across 20 technical categories (Xu et al., 2017), randomly sampled from Kaggle competition data, including technical discussions and programming queries.
- **Biomedical** contains 20,000 research paper titles across 20 scientific topics (Xu et al., 2017), sourced from BioASQ, reflecting the specialized vocabulary and structure of scientific literature.

- **GoogleNews** offers a comprehensive news perspective through 11,109 articles related to 152 events (Yin & Wang, 2016). This dataset is available in three variants: complete articles **GoogleNews-TS**, titles only **GoogleNews-T**, and snippets only **GoogleNews-S**.
- **Tweet** contains 2,472 tweets linked to 89 distinct queries (Yin & Wang, 2016), collected from the Text Retrieval Conference's microblog tracks in 2011 and 2012, reflecting the informal and concise nature of social media communication.

Datasets	**S**	N	**L**	**R**
AgNews	8000	4	23	1
SearchSnippets	12340	8	18	7
StackOverflow	20000	20	8	1
Biomedical	20000	20	13	1
GoogleNews-TS	11109	152	8	143
GoogleNews-T	11109	152	6	143
GoogleNews-S	11109	152	22	143
Tweet	2472	89	22	249

Table 4: Summary Statistics of Short-Text Datasets. S: dataset size; N: number of categories; L: average document length in words; R: ratio between largest and smallest categories.

B.2. Evaluation Metrics

Consistent with previous works (Rakib et al., 2020; Zheng et al., 2023), we employ two standard metrics to use the clustering performance: Accuracy (ACC) and Normalized Mutual Information (NMI). Accuracy measures the proportion of correct clustered texts, which is defined as:

$$ACC = \frac{\sum_{i=1}^{N} \mathbf{1}_{y_i = \text{map}(\tilde{y}_i)}}{N}, \tag{34}$$

where y_i is the true label and $\tilde{y}_i$ is the predicted label. map$(\cdot)$ function optimally aligns predicted labels with true labels using the Hungarian algorithm (Papadimitriou & Steiglitz, 1998).

Normalized Mutual Information (NMI) quantifies the shared information between the true and predicted label distributions, normalized by their individual uncertainties:

$$NMI(\boldsymbol{Y}, \tilde{\boldsymbol{Y}}) = \frac{I(\boldsymbol{Y}, \tilde{\boldsymbol{Y}})}{\sqrt{H(\boldsymbol{Y})H(\tilde{\boldsymbol{Y}})}} \tag{35}$$

where $\boldsymbol{Y}$ represent the true label sets, $\tilde{\boldsymbol{Y}}$ represent the predict label sets, I denotes mutual information, and H represents entropy. argmax(p)

B.3. Experiment Settings

The output dimension of the Encoder is $D_1 = 768$, and the output dimension of the Projection network is $D_2 = 128$. The temperature parameters for attention loss and instance-level contrastive learning loss are set to $\tau_A = 1$ and $\tau_I = 1$. The maximum sentence length of the SBERT is 32. The outer loops of the GCG algorithm T_1 and the iterations of the Lagrange multiplier algorithm T_2 are set to 10. The batch size B is 200. The total number of training iterations E_{total} is 2,000. The number of warm-up iterations E_{warm} is 600 for all datasets except Stackoverflow and Biomedical, in which we did not perform Warm-up. We built our model using PyTorch and conducted all experiments on a NVIDIA GeForce RTX 3090 Ti GPU. The number of parameters in our model is 68.4M, and the training time for different datasets varies, ranging from 10 to 30 minutes.

C. Comparison of Pseduo-labeling Effectiveness

To demonstrate the effectiveness of our proposed AEOT-based pseudo-labeling method (**AEOT-based**), we conducted comparative experiments with prediction-based pseudo-labeling method (**Predic-based**) and conventional optimal transport pseudo-labeling method (**COT-based**) using the **SearchSnippets**, **StackOverflow** and **GoogleNews-TS** datasets.

The results presented in Table 5. It can be observed that: (1) **Predicted-based** method generates pseudo-labels with lower quality because it independently assigns pseudo-labels to each sample. (2) **COT-based** method produces pseudo-labels better than the Predicted-based method by considering the global sample-to-cluster structure. However, the COT-based methods lack inherent sample-to-sample semantic consistency resulting in suboptimal pseudo-label quality. (3) Our proposed **AEOT-based** method generates the most reliable pseudo-labels duo to simultaneously consider sample-to-sample semantic consistency and sample-to-cluster global structure.

Datasets	Method	ACC	NMI
SearchSnippets	Predicted-based	72.43	59.42
	COT-based	76.81	63.82
	AEOT-based	**78.22**	**65.11**
StackOverflow	Predicted-based	69.18	63.54
	COT-based	79.63	69.78
	AEOT-based	**83.84**	**72.21**
GoogleNews-TS	Predicted-based	69.18	63.54
	COT-based	78.34	88.88
	AEOT-based	**81.32**	**90.07**

Table 5: Comparison results of different pseudo-labeling methods. Where COT-based is Eq. (16) removes the semantic regularity term $\langle \boldsymbol{S}, \boldsymbol{Q}\boldsymbol{Q}^T \rangle$.

Furthermore, to provide a more detailed comparison of the various pseudo-labeling methods, we visualize their coupling matrices during pseudo-label generation using the **StackOverflow** dataset. The "coupling matrix" refers to the predicted probability assignment matrix in the **Predicted-based** experiment, while the "coupling matrix" denotes the transport matrix in the **COT-based** and **AEOT-based** experiments. We randomly selected five samples from each of the twenty categories in the datasets for experimentation. Each consecutive group of five samples belongs to the same category.

The results illustrated in Figure 6, we can find that: (1) **Predicted-based PL** method produces incorrect soft-labels for some samples. (2) **COT-based PL** method exhibits ambiguity for some samples, where the value of the soft-labeling probability for the correct category is not predominantly high, indicating assignment uncertainty. (3) **AEOT-based PL** reduces ambiguous predictions, confidently assigning pseudo-labels to each sample, which demonstrates the superiority of our proposed pseudo-labeling approach.

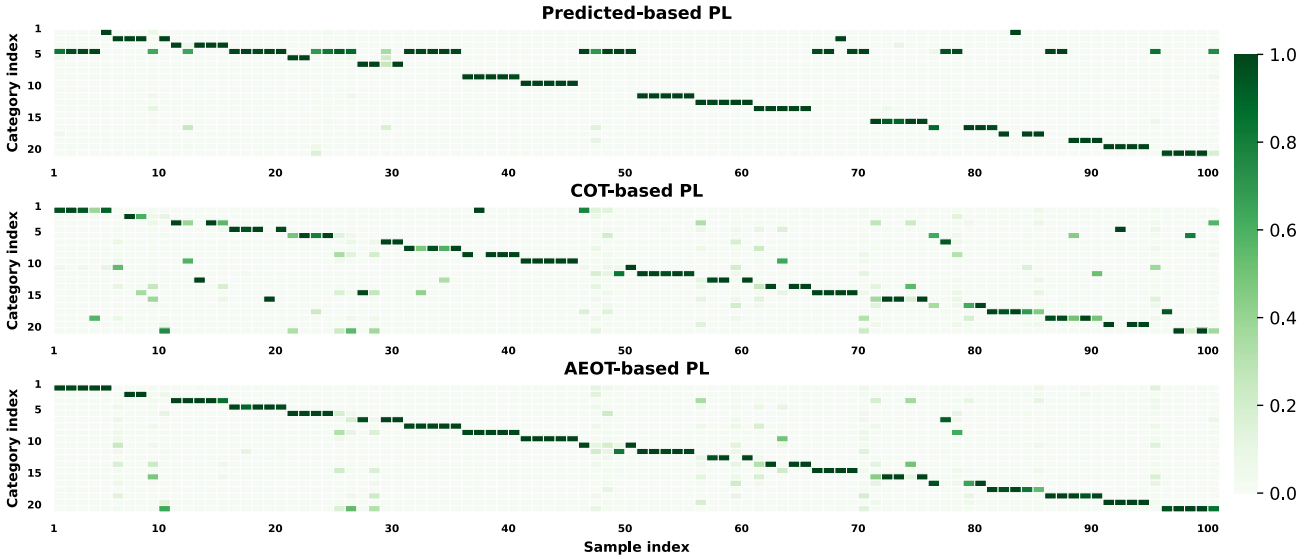

Figure 6: Coupling matrix visualization on StackOverflow. The x-axis represents the sample index, while the y-axis represents the category index. Each column represents the soft-label of the corresponding sample in the coupling matrix.

C.1. Ablation Studies

In this section, we conduct an ablation study to investigate the importance of instance-level and cluster-level contrastive learning. As mentioned in section 3.5, each level of contrastive learning plays a crucial role. To verify this, we performed ablation experiments by removing instance-level and cluster-level contrastive learning, i.e., **No IL** and **No CL**. In the **No CL** experiment, the Clustering network G_p has not received any training, so it cannot be used for clustering. Therefore, we perform clustering using K-means algorithm. The results are presented in Table 6, clearly indicating that both types of contrastive learning make significant contributions to learning effective representations, playing indispensable roles in our model's performance.

Datasets	Method	ACC	NMI
SearchSnippets	POTA	**80.12**	**67.4**
	No IL	56.65	30.66
	No CL	79.13	67.32
StackOverflow	POTA	**85.96**	**75.43**
	No IL	80.51	71.74
	No CL	61.89	57.17
GoogleNews-TS	POTA	**83.53**	**93.15**
	No IL	75.12	90.26
	No CL	77.77	92.27

Table 6: Ablation Study on two level contrastive learning.

D. Hyperparameter Analysis

We conducted a series of comprehensive experiments to validate the effects of ε_1, ε_2, ε_3 and λ with values in $\{0.1, 0.25, 0.5, 0.75, 1\}$, $\{0.6, 1.2, 5, 10, 10000\}$, $\{10, 20, 25, 30, 40\}$ and $\{1, 3, 5, 7, 10\}$, respectively. We use **AgNews**, **GoogleNews-T** and **Tweet** datasets, which represent datasets with varying levels of imbalance.

The results are presented in Figure 7. Figure 7(a), Figure 7(c) and Figure 7(d) shows that the performance of the model is almost unaffected by ε_1, ε_3 and λ, indicating that the model is insensitive to these parameters. Figure 7(b) emphasizes the importance of adjusting ε_2 on datasets with varying imbalance levels. Since this hyperparameter controls the penalty strength for the imbalance levels of predicted cluster probabilities in Eq. (16), it should be tailored to the specific imbalance level of each dataset; therefore, we set it based on the level of imbalance in the dataset.

Although our model has many hyperparameters, only ε_2 influences its performance across different types of datasets. Therefore, the model has higher adaptability when applied to unseen data. Experientially, we set $\varepsilon_1 = 1$, $\varepsilon_3 = 25$ and $\lambda = 5$ for all datasets; $\varepsilon_2 = 100$, 3.5, 0.06 and 0.03 for balanced datasets, slight imbalanced datasets, imbalanced datasets and severely imbalanced datasets, respectively.

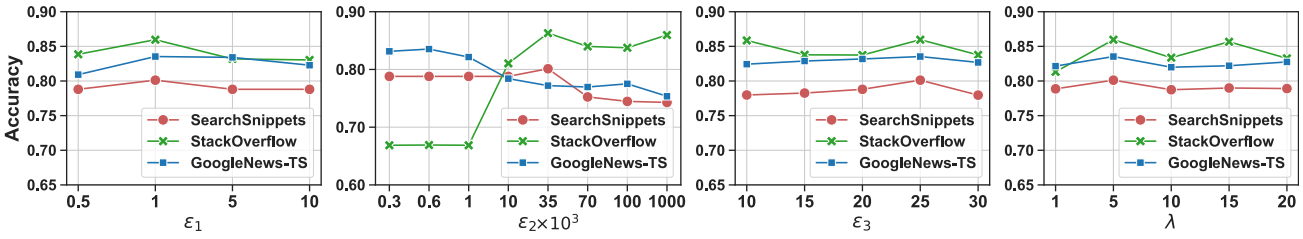

(a) Effets of ε_1 (b) Effets of ε_2 (c) Effets of ε_3 (d) Effets of λ

Figure 7: The effect of ε_1, ε_2, ε_3, and λ on model accuracy.